Water Structure at Aqueous Solution Surfaces of Atmospherically Relevant Dimethyl Sulfoxide and Methanesulfonic Acid Revealed by Phase-Sensitive Sum Frequency Spectroscopy

Xiangke Chen and Heather C. Allen*

The Ohio State University, Department of Chemistry, 100 West 18th Avenue, Columbus, Ohio 43210, United States

Interfacial water structures of aqueous dimethyl sulfoxide (DMSO) and methanesulfonic acid (MSA) were studied by Raman, infrared, and conventional and phase-sensitive vibrational sum frequency generation (VSFG) spectroscopies. Through isotopic dilution, we probed bulk water hydrogen bonding strength using the vibrational frequency of dilute OD in H_2O. As indicated by the frequency shift of the OD frequency, it is shown that DMSO has little influence on the average water hydrogen bonding strength at low concentrations in contrast with an overall weakening effect for MSA. For the water structure at the surface of aqueous solutions, although conventional VSFG spectra suggest only slight structural changes with DMSO and a red shift of hydrogen-bonded water OH frequency, phase-sensitive VSFG reveals more thoroughly structural changes in the presence of both DMSO and MSA. In the case of DMSO, reorientation of interfacial water molecules with their hydrogens pointing up toward the oxygen of the S=O group is observed. For MSA, the interfacial water structure is affected by both the dissociated methanesulfonate anions and the hydronium ions residing at the surface. Both the methanesulfonate anions and the hydronium ions have surface preference; therefore, the electric double layer (EDL) formed at the surface is relatively thin, which leads to partial reorientation of interface water molecules with net orientation of water hydrogens up. Surface DMSO molecules are more effective at reorienting surface water relative to MSA molecules.

Introduction

Tropospheric sulfur-containing aerosols play an important role in atmospheric chemistry and climate.[1–3] Especially in the marine boundary layer (MBL), the sulfur cycle dominates in the gas-to-particle conversion process and in the growth of aerosols because of the large source of biogenic dimethyl sulfide (DMS) produced by metabolic processes of algae.[4–6] Various forms of sulfur species, such as the stable intermediates dimethyl sulfoxide (DMSO) and methanesulfonic acid (MSA) and the final oxidation product H_2SO_4 are generated during the atmospheric sulfur cycle.[7–9] Because of the strong ability of these molecules to associate water, the sulfur-containing aerosols can serve as cloud condensation nuclei, impacting the formation of clouds and thereby modifying the earth's albedo and the climate.[1,3,10]

The DMSO−water mixture represents one of the more complicated binary systems because strong interactions occur not only between the molecules of a single component but also between components. Even the hydrogen-bonding properties of pure water alone are not completely understood.[11] Early studies of bulk DMSO−water mixtures presented various results, and some do not appear consistent with each other.[12–15] It has been suggested that the addition of a small amounts of DMSO to water (1) can increase the molecular ordering of water at low concentrations,[12,13] (2) has little effect on the hydrogen bond of water,[14] and (3) results in "structure breaking" of water.[15] From DMSO-rich to dilute solutions, a red-shift trend was observed for ν_b, ν_d, and ν_w (OH bonded, OH dibonded, and OH weakly bonded, respectively) in Raman spectra, revealing a disruption of long-range ordering of the water hydrogen-bonding network.[15]

Despite different views on the water structure of DMSO-perturbed solutions, it is well accepted that DMSO can form strong hydrogen bonds with water as a hydrogen bond acceptor. The hydrogen bond between DMSO and water is stronger than the hydrogen bond between water molecules.[16,17] The strong hydrogen bonds formed between DMSO and water are evidenced by the red shift of the DMSO S=O stretching frequency with increasing water concentration.[18] The two electron lone pairs on the DMSO oxygen can accept hydrogens from water molecules, which causes the red shift of the S=O frequency.

The MSA−water binary solution is less studied compared with DMSO−water systems. It has been shown that among the organosulfur species $DMSO_2$, DMSO, and MSA, MSA−water clusters require the least number of molecules to serve as the critical cluster for nucleation of water vapor.[6] This suggests a strong interaction between water and MSA molecules.

The growth and to some extent the formation of aerosols initiated by DMSO and MSA relate to their interactions with water vapor, which addresses the importance of understanding the perturbed interfacial water structure in addition to that of the bulk aqueous solutions. In contrast with the relatively abundant bulk information, the structure at aqueous surfaces is still not well understood because of limited surface-specific techniques. Vibrational sum frequency generation (VSFG) spectroscopy, one of the nonlinear spectroscopic methods that can probe the thin layers of the surface, was the only characterization method utilized to study the surface water structure of aqueous solutions of DMSO and MSA.[19–22] The VSFG spectra of the water hydrogen-bonding region (3000 to

* To whom correspondence should be addressed. E-mail: allen@chemistry.ohio-state.edu.

3600 cm^{-1}) showed, as compared with the neat water surface, slight changes induced by DMSO[22] and a significant red shift induced by MSA.[21] This was interpreted that DMSO molecules incorporate into the hydrogen bonding network and cause minimal change of the surface water structure, whereas MSA molecules enhance the hydrogen-bonding of surface water molecules.

However, as is shown in this work, the interpretation of VSFG water spectra is sometimes misleading without the phase information (net polar orientation) of the vibrational modes.[23] The recently developed phase-sensitive vibrational sum frequency generation (PS-VSFG) methods[23−25] have firmly demonstrated the ability to reveal not only the energetic states of vibrational modes but also the net polar orientation, which can greatly clarify the controversial issues in VSFG spectra interpretation.

In this article, both conventional VSFG and PS-VSFG methods are employed to present a comprehensive study of the air/aqueous interface of DMSO and MSA solutions, revealing new information on the interfacial water structure and absolute orientation of the water molecules in the interfacial region. Water structure is elucidated at relatively low solute concentrations to explore the hydrogen-bonding character and orientation of the water in different spectral regions. Typical solute concentrations used in this study are 0.02x (mole fraction, ~1 M), 0.04x (~2 M) and 0.1x (~5 M). VSFG spectra are denoted as conventional VSFG spectra, whereas phase-sensitive VSFG spectra are denoted as Im $\chi^{(2)}$ spectra.

Experimental Section

Materials. DMSO and MSA (>99% purity) were purchased from Fisher. Deionized water (not purged of CO_2) with a resistivity of 18.2 MΩ·cm and a measured pH of 5.5 was from a Barnstead Nanopure system. Deuterated water (D_2O, >99% purity) was obtained from Cambridge Isotope. Concentrations are reported in units of mole fraction denoted as x and molarity denoted as M.

VSFG and PS-VSFG Spectroscopy. The setup of our SFG systems is detailed elsewhere.[26−28] In brief, the broad bandwidth VSFG system consists of two 1 kHz repetition rate regenerative amplifiers (Spectra-Physics Spitfire, femtosecond and picosecond versions), both of which are seeded by sub-50 fs 792 nm pulses (the wavelength is tuned for system optimization) from a Ti/sapphire oscillator (Spectra-Physics, Tsunami) and pumped by a 527 nm beam from an all solid-state Nd/YLF laser (Spectra-Physics, Evolution 30). The two regenerative amplifiers provide 85 fs pulses and 2 ps pulses at 792 nm. The spectrally broad femtosecond pulses are used to drive the infrared (IR) generation in an OPA (optical parametric amplifier; TOPAS, Quantronix), and the IR energies were ~11 μJ in the O−H stretching region in the sample stage.

In the conventional VSFG setup, the intensity of the reflected sum frequency signal, I_{SF}, is proportional to the absolute square of the effective second-order susceptibility, $\chi_{eff}^{(2)}$, and to the visible and IR pulse intensities, as shown in eq 1[29]

$$I_{SFG} \propto |\chi^{(2)}|^2 I_{vis} I_{IR} \propto |\chi_{NR}^{(2)} + \sum_\nu \chi_\nu^{(2)}|^2 I_{vis} I_{IR} \quad (1)$$

with

$$\chi_\nu^{(2)} = \frac{A_\nu}{\omega_{IR} - \omega_\nu + i\Gamma_\nu} \quad (2)$$

where I_{SFG}, I_{vis}, and I_{IR} are the intensities of output SFG, incident visible, and IR pulsed laser beams. $\chi_{NR}^{(2)}$, $\chi_\nu^{(2)}$, and $\chi^{(2)}$ are the nonresonant, resonant and total second-order nonlinear susceptibilities, respectively. The resonant enhancement occurs when the frequency of the incident IR is resonant with a vibrational mode of a molecule. A_ν is the transition moment strength, ω_{IR} is the incident IR frequency, ω_ν is the frequency of the vibrational transition, and Γ_ν is the line width of the vibrational transition.

While in heterodyne-detected PS-VSFG, the Im $\chi^{(2)}$ spectra contain information of the sign of the second-order nonlinear susceptibility, as shown in eq 3

$$\text{Im } \chi^{(2)} = -\sum_\nu \frac{A_\nu \Gamma_\nu}{(\omega_{IR} - \omega_\nu)^2 + \Gamma_\nu^2} \quad (3)$$

The VSFG spectrum is polarization-dependent. In this study, spectra with the polarization combination of ssp (s-SFG, s-visible, p-infrared) are shown. The VSFG spectra were normalized against a nonresonant VSFG spectrum from a GaAs crystal (Lambda Precision Optics) to remove the spectral distortion caused by the energy profile of the IR pulse. To calibrate the VSFG peak positions, we used the VSFG spectrum containing polystyrene IR absorption bands.

For PS-VSFG, our broad bandwidth VSFG system was redesigned. A 300 μJ visible beam (s-polarized, 792 nm) and a ~11 μJ IR beam (p-polarized, OH stretch region) were spatially and temporally overlapped at incident angles of 50 and 60° on sample stage 1 (for samples and z-cut quartz), respectively. The visible, IR, and generated sum frequency (s-polarized) beams reflected from sample stage 1 were refocused by a gold concave mirror (f = 100 mm) onto a GaAs (Lambda Precision Optics) surface on sample stage 2 to generate another sum frequency beam (local oscillator, LO). The sum frequency beam from sample stage 1 was delayed ~2.5 ps by passing through an ~1 mm thick silica plate positioned before the gold concave mirror. The time difference between the sum frequency beams from two sample stages introduced an interference fringe in the frequency domain. This interferogram was stretched in a monochromator (Acton Research, SpectraPro SP-500 monochromator with a 1200 g/mm grating blazed at 750 nm) and then detected by a liquid-nitrogen cooled charge-coupled device (CCD) (Roper Scientific, 1340 × 400 pixel array, LN400EB back-illuminated CCD). The height of the sample surface, which is critical for accurate phase determination, is also checked by the image on the CCD. Final spectra are processed from the raw interferograms through Fourier transformation.[28]

Raman and Transmission IR Spectra. Raman spectra were obtained by passing a ~200 mW 532 nm light source (Raman System) from a continuous wave laser onto the sample and then detecting in a 90° direction. The incident 532 nm light was focused by a 7.5 mm Raman probe (InPhotonics), and the scattered light was focused onto the entrance slit of a 500 mm monochromator (Acton Research, SpectroPro SP-500), dispersed by a 1200 groove/mm grating blazed at 1 μm, and then collected on a liquid-nitrogen-cooled CCD camera (Roper Scientific, LN400EB). Transmission IR measurements were performed on a Perkin-Elmer IR microscope system with CaF_2 windows and a liquid-nitrogen-cooled MCT detector.
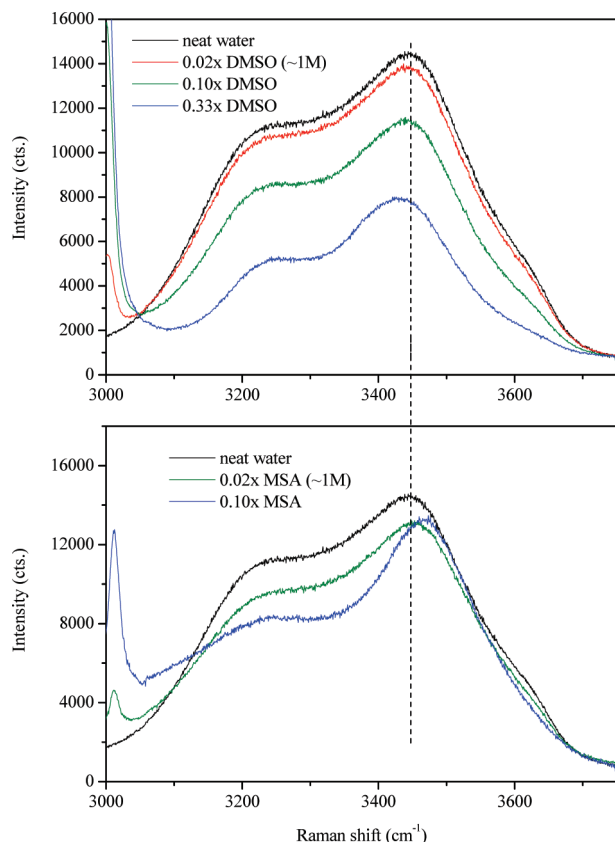
Water Structure at Aqueous Solution Surfaces

J. Phys. Chem. B, Vol. 114, No. 46, 2010 **14985**

Figure 1. Water stretch region Raman spectra of a series of DMSO−water (top) and MSA−water mixtures (bottom).

Results and Discussion

Bulk Water Structure of Aqueous DMSO/MSA Solutions. Before discussing the influence of DMSO and MSA on the interfacial water structure, it is helpful to investigate the structural change of water in bulk solutions. Spectroscopic methods such as IR and Raman have been extensively used to reveal the water structure, hydrogen-bonding properties, and the hydrated structure around solutes. Although much work has been done, structural understanding is still incomplete.

The Raman spectra of water and aqueous DMSO and MSA solutions are shown in Figure 1 and are consistent with previously published Raman data.[15] The main spectral feature of neat water is the bimodal shape centered at ∼3220 and ∼3440 cm^{-1}, with a slight but detectable high-frequency shoulder around 3630 cm^{-1}. Questions arise on how to interpret the water spectra as some try to fit the spectra with several Gaussians and attribute each to a particular molecular environment,[15,30] whereas others view liquid water as a dynamical continuum with the spectra complicated by intramolecular and intermolecular vibrational couplings.[31,32] Upon the addition of DMSO or MSA to the water, the bimodal spectral shape remains with a decrease in overall intensity due to less water content. Upon closer examination of the DMSO spectra, there is no change in the band positions up to 0.1x, and the bimodal shape becomes narrower at 0.33x DMSO. In contrast, a blue shift of the 3440 cm^{-1} peak is observed in the presence of 0.1x MSA, and the baseline of the low frequency side is clearly elevated. The spectral narrowing at relatively high DMSO concentration can arise from either the DMSO−water interaction or the reduced coupling between water molecules because of less water concentration. However, the blue shift of the OH stretch frequency in aqueous MSA seems to imply a weakening of the
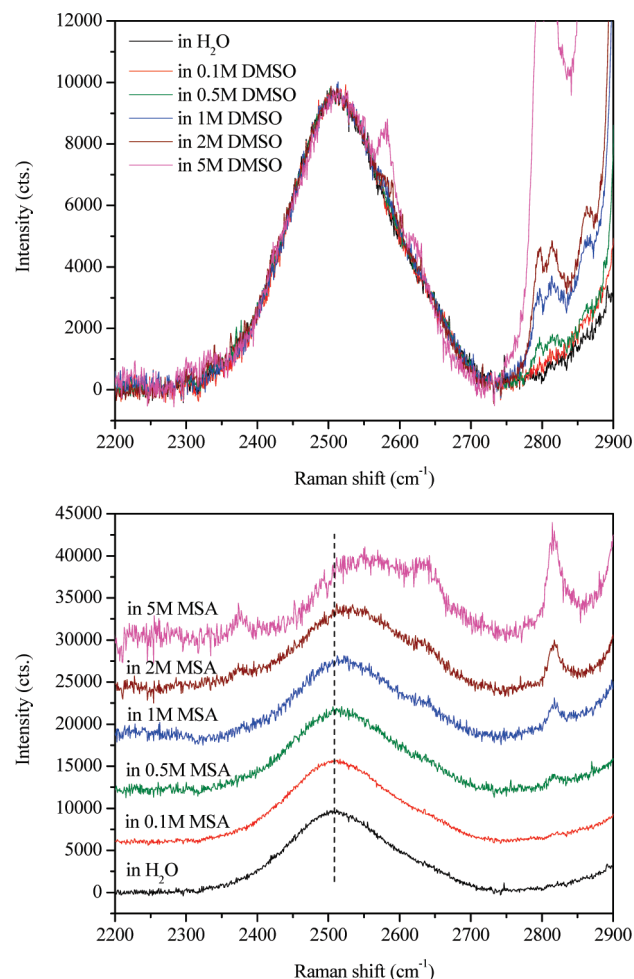

Figure 2. O−D stretch region Raman spectra of dilute OD (D$_2$O/H$_2$O 4:96) in DMSO−H$_2$O (top) and MSA−H$_2$O mixtures (bottom).

water hydrogen-bonding network. In addition, the broad continuum that causes the baseline lift indicates the existence of hydrated hydronium ions,[33] confirming the dissociation of MSA at this concentration.

Spectra of isotopically diluted water, in particular, the dilute HOD in H$_2$O, are simplified because most of the intramolecular and intermolecular vibrational couplings of the OD stretch to other vibrational modes are minimized.[11,31,32] As a result, the decoupled OD stretch displays a monomodal shape and can be used as a sensitive local probe for the water structure. The most important information from the HOD spectra is that of the OD peak position, which is considered to be empirically proportional to the hydrogen bond strength.[34] Figure 2 shows the Raman spectra of the OD stretch in the presence of DMSO and MSA up to 5 M concentration (∼0.1x). As expected from the slight change observed for purely H$_2$O spectra with DMSO, both the band position and the width of the OD stretch show no change for all DMSO concentrations studied (0.1 to 5 M). The small sharp peaks that overlaid on the OD stretch are from the DMSO CH$_3$ vibrations. These spectra are consistent with previous studies[14] and indicate that DMSO forms strong hydrogen bonds with water that are similar in strength to those of water−water interactions. Therefore, accommodation of a relatively low amount of DMSO into the water hydrogen-bonding network should not significantly change the energetic states of the overall water hydrogen bonds. This observation does not necessarily contradict with the ordering of water molecules at low DMSO concentrations. An increase in the radial distribution function
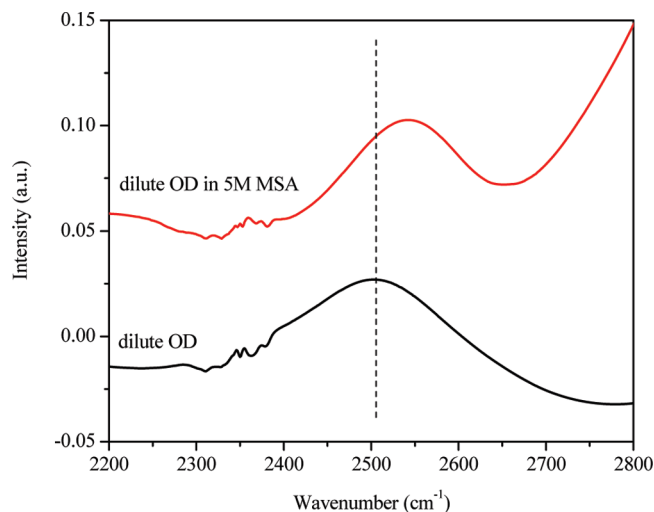
Figure 3. Transmission IR absorption spectra of dilute OD (D_2O/H_2O 4:96) in MSA−H_2O mixtures.

(RDF) intensity showed ordering in the spatial arrangement of oxygen atoms, whereas the strength of individual hydrogen bonds was suggested to remain almost unchanged.[13,14]

By adding MSA, a similar blue shift of the OD stretch is observed at 5 M ($\sim 0.1x$), as in the H_2O spectra of Figure 1. Because MSA is mostly dissociated into hydrated ions at this concentration, the OD spectra should be considered as "cation + anion affected" water spectra.[34] The water structure affected by other cations and anions has been systematically studied using HOD spectra.[34,35] Terms like "structure makers" and "structure breakers" continue to be commonly used to describe the impact of solutes on water hydrogen bond strength based on the red shift and blue shift of the OD frequency, respectively. Structure making and breaking refers to the structure of water around the solute. The OD peak position was found to be correlated with surface charge density of the cations.[34,35] Typically, the affected OD peak occurs at higher frequency by monovalent metal cations and at lower frequency by divalent or trivalent metal cations. Hydronium ion, because of its high surface charge density, was shown to cause a red shift on the OH/OD stretch frequency and thus was considered to be a "structural maker".[36] Many anions, especially large species such as ClO_4^- are typically termed "structural breakers" and cause a blue shift of the OD stretch frequency.[34] The OD stretch in MSA blue shifts from $\sim$2510 to $\sim$2550 cm^{-1}, which coincidences with the OD frequency shift caused by methanesulfonate anion ($CH_3SO_3^-$).[34] Therefore, the overall hydrogen bond strength of dilute OD is weakened by $0.1x$ MSA, which is mainly due to the hydrated methanesulfonate anion through ion−dipole interaction. The OD stretch shift caused by MSA is observed not only in Raman spectra but also in FT-IR absorption spectra, as shown in Figure 3.

Surface Water Structure of Aqueous DMSO/MSA Solutions. The different interaction mechanism of DMSO and MSA with water will certainly alter the surface water structure because of their notable surface preference.[19,21] The VSFG spectra in the water stretch region of 1 ($\sim 0.02x$) and 2 M ($\sim 0.04x$) DMSO and MSA are shown in Figure 4. Our conventional VSFG spectra of neat water and aqueous DMSO and MSA solutions agree well with previous studies.[19−22] Our PS-VSFG data shown in Figure 5 are the first to be published, however, for these systems.

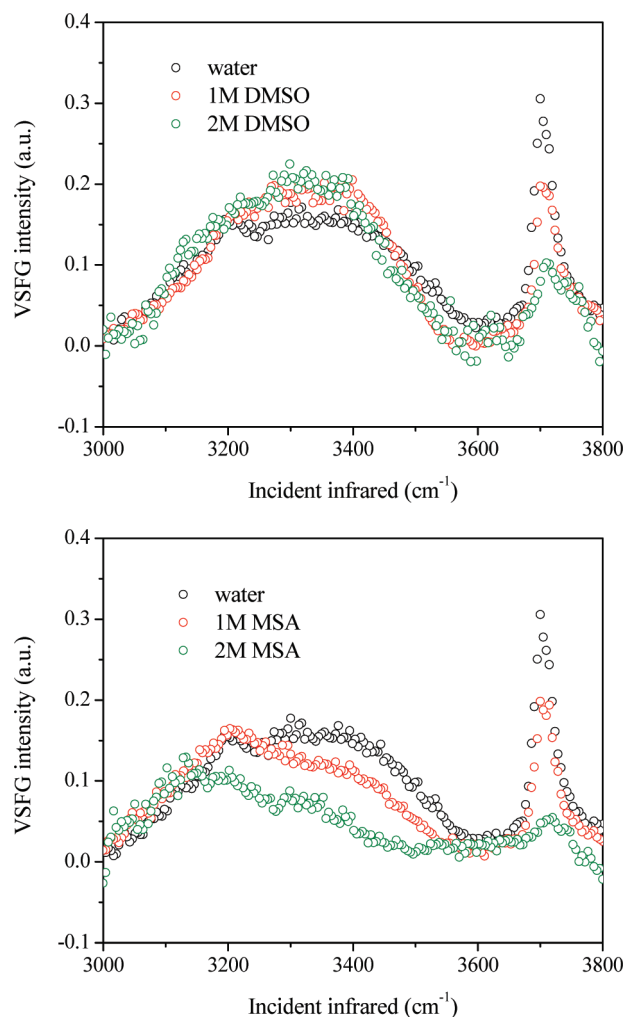For conventional VSFG neat water spectra, the unbound dangling OH stretch manifests as a sharp peak at 3700 cm^{-1},

Figure 4. Conventional VSFG spectra in water stretch region of DMSO−water mixtures (top) and MSA−water mixtures (bottom).
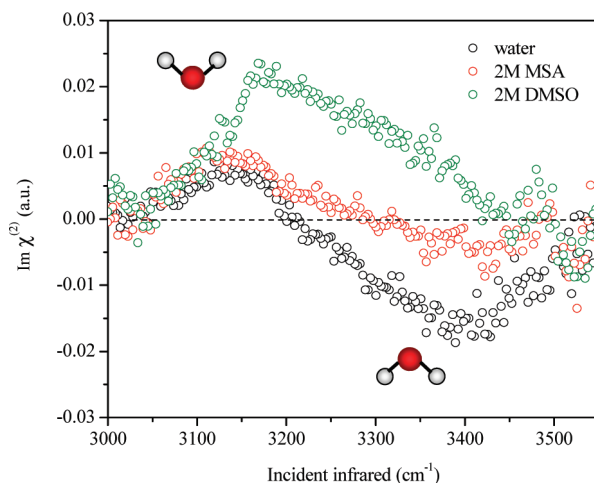

Figure 5. Im $\chi^{(2)}$ spectra in water region of 2 M DMSO, 2 M MSA, and neat water. In Im $\chi^{(2)}$ water spectra, positive bands correspond to a net pointing up of hydrogens of OH bonds, whereas negative bands correspond to OH hydrogens pointing down into bulk, as shown by the inset water molecule scheme.

and the hydrogen-bonded OH stretch is observed in bimodal shape between 3000 and 3600 cm^{-1}. Similar to bulk water, the interpretation of the VSFG spectra of the hydrogen-bonded region has not been fully agreed upon. The two characteristic bands centered at $\sim$3200 and $\sim$3400 cm^{-1} are commonly

labeled as "ice-like" and "liquid-like" water structures owing to their spectral similarity with the bulk ice and liquid water.[37] Other assignments such as "strongly/weakly hydrogen bonded" or "symmetrically/asymmetrically 4-coordinated" water structures are also mentioned.[38,39]

For the dangling OH region, a decrease in intensity is observed for 1 M DMSO and MSA solutions. This decrease becomes much more obvious for 2 M DMSO and MSA concentration, suggesting that the topmost water molecules are replaced or hydrogen bonded by solutes. The perturbation of DMSO and MSA on the dangling OH is very different from the effect of several other solvated ions, for example, OH^-, Na^+, and halogen anions, which leave the dangling OH little changed.[40–42] This difference should arise from the hydrophobic CH_3 moieties of DMSO and MSA, which lead to their preferential existence at the outermost surface. Previous MD simulations also suggested the free OH decrease with increasing DMSO concentration.[43]

The VSFG spectra of the hydrogen-bonded region of aqueous DMSO and MSA in Figure 4 are quite different. The change in this region induced by DMSO seems to be small. The 3200 cm^{-1} band is little affected, which was explained by the incorporation of DMSO into the interfacial water and the preservation of the hydrogen-bonding environment. The slightly increased intensity near $\sim$3300 cm^{-1} was attributed to a strengthened hydrogen bonding environment due to strong DMSO−water interactions.[22] On the contrary, a significant decrease in the hydrogen-bonded region, especially the 3400 cm^{-1} band, is observed for the 2 M aqueous MSA, and the overall hydrogen bonded region is somewhat red-shifted. Previously, this was explained that MSA enhances the strength of the interfacial hydrogen-bonding network.[21]

However, because the conventional VSFG intensity is proportional to the absolute square of the nonlinear susceptibility, $|\chi^{(2)}|^2$, the phase (polar orientation) giving rise to each band and its interference is not known and is subject to arbitrary fitting procedures. Therefore interpretation of water structure based on conventional VSFG spectra is less informative and can be incorrect.[24,44] Recently, PS-VSFG methods have been developed on both scanning SFG and broad bandwidth SFG systems.[24,25] In PS-VSFG spectra, the imaginary part of $\chi^{(2)}$ is obtained, hence giving information on the net polar orientation on the isotropic liquid surface. Figure 5 shows the Im $\chi^{(2)}$ spectra in the hydrogen-bonded region of neat water and 2 M aqueous DMSO and MSA. Remarkable differences are revealed as compared with the conventional VSFG spectra and are discussed below.

The assignment of Im $\chi^{(2)}$ spectrum of neat water has been suggested by Shen and coworkers;[24] the negative region from 3450 to 3600 cm^{-1} has been assigned to donor-bonded OH stretches of three-coordinate DDA and DAA water molecules in the topmost layer. (Here D and A denote donor and acceptor hydrogen bonds, respectively, with which water molecules hydrogen bond to nearest neighbors.) The negative region from 3200 to 3450 cm^{-1} has been assigned to loosely hydrogen-bonded four-coordinate DDAA molecules, whereas the positive region from 3000 to 3200 cm^{-1} was mainly attributed to strongly hydrogen-bonded DDAA molecules. The above assigned spectral regions overlap with each other, which leads to a crossover point around 3200 cm^{-1}. The negative sign in an Im $\chi^{(2)}$ spectrum that reveals phase corresponds to the OH stretches with a net orientation of the hydrogens pointing down toward the bulk, and the positive sign corresponds to a net orientation with hydrogens pointing up.

For 2 M aqueous DMSO, the surface water structure is greatly changed despite the resemblance of the conventional VSFG spectra. As seen in Figure 5, the sign of OH stretch becomes positive throughout the hydrogen-bonded region in 2 M aqueous DMSO, revealing a net up orientation of water dipoles (pointing from oxygen to hydrogen). That is, the presence of sufficient DMSO molecules at the surface reorients the loosely hydrogen-bonded DDAA molecules at surface. This reorientation should be directly related to the hydrogen bond formed between DMSO and water. As previously shown,[19,43] DMSO molecules exhibit surface preference with the CH_3 groups pointing up and the S=O group pointing slightly inward. Water fraction at the topmost layer is therefore greatly reduced. To form hydrogen bonds with the oxygen on S=O moiety at the topmost layer, part of interfacial water molecules thus need to reorient and point with their hydrogen up to the DMSO oxygen. The reorientation of water molecules under perturbation of DMSO was suggested in a previous VSFG study.[22]

The Im $\chi^{(2)}$ spectrum of 2 M MSA is also interesting, with the positive band below 3200 cm^{-1} less affected and the negative band around 3400 cm^{-1} near zero. Surface water structure is perturbed by both the hydrated methanesulfonate anion and the hydrated hydroniums. The resulting Im $\chi^{(2)}$ spectrum, however, appears like neither anion-affected nor hydronium-ion-affected Im $\chi^{(2)}$ spectra.[28,42] For the Im $\chi^{(2)}$ spectra of water in the presence of anions at the outmost surface, that is, deprotonated fatty acid, the sign of the overall hydrogen bonded region is all positive, as dictated by the surface anions.[28] On the contrary, for acidic HCl and HI solutions, the sign of the overall hydrogen-bonded region is all negative in Im $\chi^{(2)}$ spectra,[42] suggesting that hydronium ions have more surface excess than the halogen anions and thus create a surface field inducing the OH to point down. In the case of MSA, both the methanesulfonate anion and the hydronium ion have surface preference as compared with the bulk. However, the methanesulfonate anions should have more surface propensity and therefore excess relative to the hydronium ions, as evidenced by their relative impact on the dangling OH, as shown in previous studies.[19–21,36,42,45] Overall, the surface methanesulfonate anions tend to orient interfacial water molecules with their dipoles pointing up, which, however, are partially offset by the hydronium ions at the surface. The resultant surface electric double layer (EDL) is thin, and the overall conventional VSFG and PS-VSFG spectral intensities are low.

Conclusions

A comprehensive investigation of the water structure at the aqueous DMSO and MSA surfaces was completed. The results imply that both DMSO and MSA molecules have surface preference that decreases the dangling OH fraction at the surface. For surface DMSO molecules, the S=O group at the surface forms strong hydrogen bonds with water, which results in reorientation of interfacial water molecules with their hydrogens pointing up toward the oxygen of the S=O group. MSA molecules completely dissociate into hydrated ions at low concentrations ($<0.1x$), and the interfacial water structure is therefore affected by both the methanesulfonate anions and the hydronium ions residing at and near the surface. The EDL in the interface formed by the methanesulfonate anions and the hydronium ions is relatively small and thereby only minimally orients water molecules with their hydrogens up. Reorientation of water caused by DMSO is stronger than that caused by MSA.

References and Notes

(1) Charlson, R. J.; Lovelock, J. E.; Andreae, M. O.; Warren, S. G. *Nature* **1987**, *326*, 655–661.

(2) Andreae, M. O.; Crutzen, P. J. *Science* **1997**, *276*, 1052–1058.

(3) von Glasow, R.; von Kuhlmann, R.; Lawrence, M. G.; Platt, U.; Crutzen, P. J. *Atmos. Chem. Phys.* **2004**, *4*, 2481–2497.

(4) Schwartz, S. E. *Nature* **1988**, *336*, 441–445.

(5) Wakeham, S. G.; Dacey, J. W. H. *ACS Symp. Ser.* **1989**, *393*, 152–166.

(6) Debruyn, W. J.; Shorter, J. A.; Davidovits, P.; Worsnop, D. R.; Zahniser, M. S.; Kolb, C. E. *J. Geophys. Res., [Atmos.]* **1994**, *99*, 16927–16932.

(7) Yin, F. D.; Grosjean, D.; Seinfeld, J. H. *J. Atmos. Chem.* **1990**, *11*, 309–364.

(8) Barone, S. B.; Turnipseed, A. A.; Ravishankara, A. R. *Faraday Discuss.* **1995**, *100*, 39–54.

(9) Schweitzer, F.; Magi, L.; Mirabel, P.; George, C. *J. Phys. Chem. A* **1998**, *102*, 593–600.

(10) Charlson, R. J.; Schwartz, S. E.; Hales, J. M.; Cess, R. D.; Coakley, J. A.; Hansen, J. E.; Hofmann, D. J. *Science* **1992**, *255*, 423–430.

(11) Auer, B. M.; Skinner, J. L. *J. Chem. Phys.* **2008**, *128*, 224511-1–224511-12.

(12) Safford, G. J.; Schaffer, P. C.; Leung, P. S.; Doebbler, G. F.; Brady, G. W.; Lyden, E. F. X. *J. Chem. Phys.* **1969**, *50*, 2140–2159.

(13) Vaisman, I. I.; Berkowitz, M. L. *J. Am. Chem. Soc.* **1992**, *114*, 7889–7896.

(14) Brink, G.; Falk, M. *J. Mol. Struct.* **1970**, *5*, 27–30.

(15) Scherer, J. R.; Go, M. K.; Kint, S. *J. Phys. Chem.* **1973**, *77*, 2108–2117.

(16) Puranik, S. M.; Kumbharkhane, A. C.; Mehrotra, S. C. *J. Chem. Soc., Faraday Trans.* **1992**, *88*, 433–435.

(17) Soper, A. K.; Luzar, A. *J. Phys. Chem.* **1996**, *100*, 1357–1367.

(18) Bertoluzza, A.; Bonora, S.; Battaglia, M. A.; Monti, P. *J. Raman Spectrosc.* **1979**, *8*, 231–235.

(19) Allen, H. C.; Gragson, D. E.; Richmond, G. L. *J. Phys. Chem. B* **1999**, *103*, 660–666.

(20) Allen, H. C.; Raymond, E. A.; Richmond, G. L. *Curr. Opin. Colloid Interface Sci.* **2000**, *5*, 74–80.

(21) Allen, H. C.; Raymond, E. A.; Richmond, G. L. *J. Phys. Chem. A* **2001**, *105*, 1649–1655.

(22) Tarbuck, T. L.; Richmond, G. L. *J. Phys. Chem. B* **2005**, *109*, 20868–20877.

(23) Shen, Y. R.; Ostroverkhov, V. *Chem. Rev.* **2006**, *106*, 1140–1154.

(24) Ji, N.; Ostroverkhov, V.; Tian, C. S.; Shen, Y. R. *Phys. Rev. Lett.* **2008**, *100*, 096102−096105.

(25) Nihonyanagi, S.; Yamaguchi, S.; Tahara, T. *J. Chem. Phys.* **2009**, *130*, 204704-1–204704-5.

(26) Hommel, E. L.; Allen, H. C. *Anal. Sci.* **2001**, *17*, 137–139.

(27) Tang, C. Y.; Allen, H. C. *J. Phys. Chem. A* **2009**, *113*, 7383–7393.

(28) Chen, X. K.; Hua, W.; Huang, Z. S.; Allen, H. C. *J. Am. Chem. Soc.* **2010**, *132*, 11336–11342.

(29) Zhuang, X.; Miranda, P. B.; Kim, D.; Shen, Y. R. *Phys. Rev. B* **1999**, *59*, 12632–12640.

(30) Brubach, J. B.; Mermet, A.; Filabozzi, A.; Gerschel, A.; Roy, P. *J. Chem. Phys.* **2005**, *122*, 184509.

(31) Wall, T. T.; Hornig, D. F. *J. Chem. Phys.* **1965**, *43*, 2079–2087.

(32) Falk, M.; Ford, T. A. *Can. J. Chem.* **1966**, *44*, 1699–1707.

(33) Janosche, R.; Weideman, Eg.; Zundel, G.; Pfeiffer, H. *J. Am. Chem. Soc.* **1972**, *94*, 2387–2396.

(34) Stangret, J.; Gampe, T. *J. Phys. Chem. A* **2002**, *106*, 5393–5402.

(35) Mikenda, W. *Monatsh. Chem.* **1986**, *117*, 977–984.

(36) Tarbuck, T. L.; Ota, S. T.; Richmond, G. L. *J. Am. Chem. Soc.* **2006**, *128*, 14519–14527.

(37) Du, Q.; Superfine, R.; Freysz, E.; Shen, Y. R. *Phys. Rev. Lett.* **1993**, *70*, 2313–2316.

(38) Richmond, G. L. *Chem. Rev.* **2002**, *102*, 2693–2724.

(39) Gopalakrishnan, S.; Liu, D. F.; Allen, H. C.; Kuo, M.; Shultz, M. J. *Chem. Rev.* **2006**, *106*, 1155–1175.

(40) Liu, D.; Ma, G.; Levering, L. M.; Allen, H. C. *J. Phys. Chem. B* **2004**, *108*, 2252–2260.

(41) Mucha, M.; Frigato, T.; Levering, L. M.; Allen, H. C.; Tobias, D. J.; Dang, L. X.; Jungwirth, P. *J. Phys. Chem. B* **2005**, *109*, 7617–7623.

(42) Tian, C. S.; Ji, N.; Waychunas, G. A.; Shen, Y. R. *J. Am. Chem. Soc.* **2008**, *130*, 13033–13039.

(43) Benjamin, I. *J. Chem. Phys.* **1999**, *110*, 8070–8079.

(44) Ostroverkhov, V.; Waychunas, G. A.; Shen, Y. R. *Phys. Rev. Lett.* **2005**, *94*, 046102-1–046102-4.

(45) Levering, L. M.; Sierra-Hernandez, M. R.; Allen, H. C. *J. Phys. Chem. C* **2007**, *111*, 8814–8826.